Experimental Realization of Second Harmonic Generation in a Fibonacci Optical Superlattice of $LiTaO_3$

Shi-ning Zhu, Yong-yuan Zhu, Yi-qiang Qin, Hai-feng Wang, Chuan-zhen Ge, and Nai-ben Ming
National Laboratory of Solid State Microstructures, Nanjing University, Nanjing 210093, China
and Center for Advanced Studies in Science and Technology of Microstructures, Nanjing 210093, China
(Received 30 July 1996; revised manuscript received 10 January 1997)

We have designed and fabricated a novel nonlinear optical superlattice of $LiTaO_3$ in which two antiparallel 180° domains building blocks A and B were arranged as a Fibonacci sequence. We measured the quasi-phase-matched second-harmonic spectrum of the superlattice. The second-harmonic blue, green, red, and infrared light generation, with energy conversion efficiencies of $\sim 5\% - 20\%$, was demonstrated experimentally, which efficiencies are comparable with those of a periodic superlattice. Destruction of self-similarity and extinction phenomenon have also been observed in the spectrum. The experiment results are in good agreement with theory. [S0031-9007(97)02784-1]

PACS numbers: 42.65.Ky, 77.80.Dj, 78.66.–w

An important development in condensed-matter physics is the discovery of quasicrystalline structure [1]. Much effort has been devoted to the studies of structure and physical properties of quasicrystal [2,3]. A quasiperiodic superlattice is an analog of one-dimensional quasicrystal. The first quasiperiodic semiconductor superlattice was fabricated by Merlin *et al.* by molecular-beam epitaxy in 1985 [4]. Since then metallic and dielectric Fibonacci superlattices have been produced by various techniques [5–7]. These superlattices have shown many unusual physical properties depending on their composition and layer thickness.

In dielectric crystals, the most important physical processes are the excitation and the propagation of classical waves, including optical waves and acoustic waves. Ultrasonic excitation and propagation in the quasiperiodic acoustic superlattices have been studied both theoretically and experimentally [8]. More recently, the localization of optical waves in a quasiperiodic optical superlattice (QPOS) of SiO_2 and TiO_2 has been reported [9]. For second-order nonlinear optical effects of the QPOS, some preliminary theoretical work has been carried out [10]. It has been discovered that the second harmonic spectrum of a QPOS is different from that of a periodic optical superlattics (POS) due to its lower space-group symmetry. According to the theory of quasiphase-matching (QPM) proposed by Armstrong *et al.* [11], the phase matching condition in the second harmonic process of a QPOS can be written into

$$\Delta k = k_{2\omega} - 2k_{\omega} - G_{m,n} = 0, \qquad (1)$$

where $k_{2\omega}, k_{\omega}$ are the wave vectors of the second harmonic and fundamental waves, respectively, $G_{m,n}$ is the reciprocal vector (called the "grating wave vector" in nonlinear optics) which depends on the structure parameter of a QPOS. In a Fibonacci system, two incommensurate periods with ratio τ are superimposed. The indexing of $G_{m,n}$ requires two integers m, n, which is different from the POS's reciprocal vector G_n indexed with only one integer. Therefore, a QPOS can provide more reciprocal vectors to the QPM optical parametric process, which results in the second harmonic spectrum of a QPOS showing more plentiful spectrum structure than that of a POS. This characteristic of the QPOS may be used in multiwavelength laser frequency conversion application. However, up to now, this has not been experimentally proved due to the lack of proper material.

In this paper, we report for the first time the second harmonic generation experiment on a Fibonacci optical superlattice of $LiTaO_3$ (LT). The superlattice was fabricated by the external field poling technique at room temperature. We measured the QPM second-harmonic spectrum of the QPOS and calculated its main effective second-order nonlinear optical coefficients $d_{m,n}$. Two different extinction rules were found. We confirmed that the second-harmonic spectrum of the QPOS does not reflect the symmetry of the quasiperiodic structure due to the dispersive effect of the refractive index and, consequently, self-similarity destructs in this spectrum.

The QPOS with Fibonacci sequence is constructed as follows. We first define two fundamental blocks A and B, which are arranged according to the production rule $S_j = S_{j-1} \,|\, S_{j-2}$ with $j \geq 3$, $S_1 = A$, and $S_2 = AB$. Both block A and block B are composed of one positive and one negative ferroelectric domain, so that neighboring domains are interrelated by a dyad axis in the x direction. As illustrated in Figs. 1(a) and 1(b), l_A and l_B represent the thickness of block A and block B, respectively, where $l_A = l_{A1} + l_{A2}, l_B = l_{B1} + l_{B2}$. Let $l_{A1} = l_{B1} = l$, $l_{A2} = l(1 + \eta), l_{B2} = l(1 - \tau\eta)$, where l, η are adjustable structure parameters, $\tau = (1 + \sqrt{5})/2$ is the golden ratio. The sequence of the blocks, $ABAABABA\ldots$, produces a QPOS with $l_A/l_B = \tau$; see Fig. 1(b). Even if $l_A/l_B \neq \tau$, the quasiperiodic properties of the superlattics are still preserved. Since the second-order nonlinear-optical coefficients form a third-rank tensor, they will change their signs from positive domains to negative domains, so the nonlinear coefficients in the superlattice

 0031-9007/97/78(14)/2752(4)$10.00

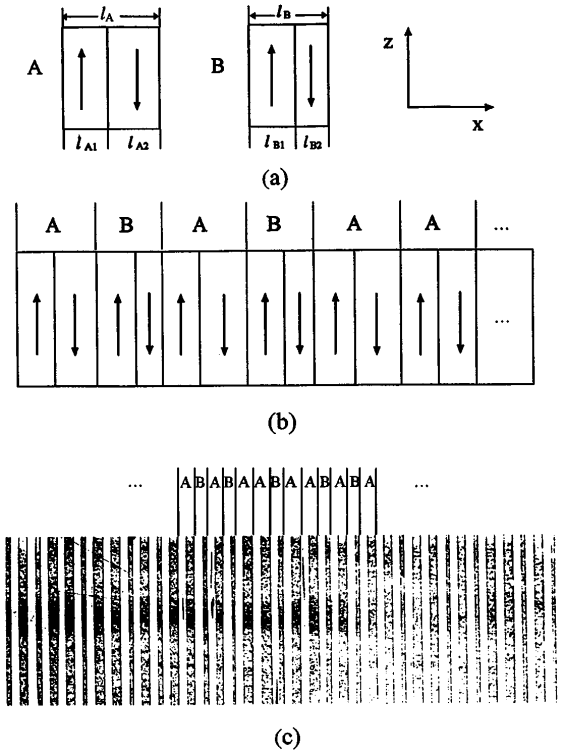

FIG. 1. Quasiperiodic optical superlattic (QPOS) made from a LT single crystal. (a) Two building blocks: A and B, each composed of one positive and one negative ferroelectric domain. (b) Schematic diagram of a QPOS with Fibonacci sequence. (c) The optical micrograph of a QPOS of LT single crystal revealed by etching.

are modulated with quasiperiodic sign reversal. In order to utilize to the largest nonlinear optical coefficient d_{33} ($= 26$ pm/V for LT), the ferroelectric domain lamellae are arranged along the x axis of the LT crystal and the domain boundaries parallel to the y-z plane, the z-polarized fundamental wave propagates along the x axis of crystal. For an infinite array, the modulated nonlinear coefficient $d(x)$ can be written by use of Fourier transform approach [10,12] as

$$d(x) = \sum_{m,n} d_{m,n} e^{iG_{m,n}x}, \tag{2}$$

where the reciprocal vector $G_{m,n} = 2\pi D^{-1}(m + n\tau)$, $D = \tau l_A + l_B$ is the "average structure parameter" of the superlattice. The corresponding Fourier coefficients $d_{m,n}$ can be defined as the effective nonlinear coefficients of the QPOS.

The sample was fabricated by poling a z-cut LT single-domain wafer at room temperature [13]. Figure 1(c) is the optical micrograph of the cross section of the poled sample revealed by etching; the observed surface was perpendicular to the y axis and the lamellae were perpendicular to the x axis. The figure shows that a volume quasiperiodic domain grating has been produced in the sample. In the QPOS block A and block B consist nominally of 11, 13 μm and 11, 6.5 μm, respectively. The sample has 13 generations (S_{13}), 377 A and B blocks, with a total length of $\sim$8 mm and a thickness of $\sim$0.5 mm.

We used a tunable optical parametric oscillator (OPO) as the fundamental light source. Its pulse duration was 23 ps and the repetition rate was 1 Hz. The fundamental wave was polarized along the z axis of the sample. It was weakly focused and coupled into the polished end face of the sample and propagated along the x axis of the sample. The radius of the waist inside the sample was $\omega_0 \approx 0.1$ mm. The confocal parameter for the system was $Z_0 \approx 6$ cm. Because Z_0 is much greater than the length of the sample, the plane-wave theory of second-harmonic generation (SHG) can be applied to the Gaussian beam.

The SHG spectrum of the QPOS of LT was measured in the range from 0.9 to 1.4 μm and from 1.55 to 1.7 μm [Fig. 2(a)], respectively. When the fundamental wavelength was tuned to 0.9726, 1.0846, 1.2834, 1.3650, and 1.5699 μm, we obtained QPM second harmonic blue, green, red, and infrared light output with conversion efficiencies up to $\sim$5%–20% (Table I). According to Eq. (1), the position of second harmonic peaks may be marked with fundamental wavelength as

$$\left[\frac{I}{\lambda}\right]_{m,n} = \frac{G_{m,n}}{4\pi[n_2(\lambda) - n_1(\lambda)]}, \tag{3}$$

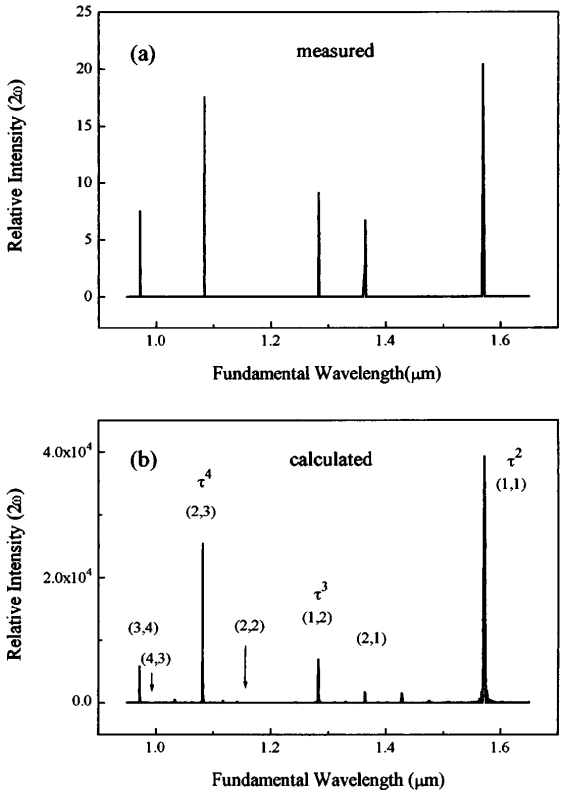

FIG. 2. The SHG spectra measured and calculated in a QPOS of LT. Note that (i) $(1/\lambda)_{1,4} \neq (1/\lambda)_{1,2} + (1/\lambda)_{1,3}$ and (ii) the $(2, 2)$ peak and $(4, 3)$ peak are absent in the spectra.

TABLE I. SHG experiment results of quasiperiodic poling $LiTaO_3$. The fundamental source is a ps-OPO with the repetition of 1 Hz and the duration of 23 ps.

Reciprocal vectors	Fundamental wavelength (μm)		Harmonic wavelength (μm)	Input	Output	FWHM	Efficiency
$G_{m,n}$	Calculated	Measured	Measured	energy (μJ)	energy (μJ)	(nm)	%
(3,4)	0.9720	0.9726	0.4863	40	3	~0.3	~7.5
(2,3)	1.0820	1.0846	0.5423	40	7	~0.4	~17.5
(1,2)	1.2830	1.2834	0.6417	33	3	~0.85	~9.1
(2,1)	1.3640	1.3650	0.6825	30	2	~1.1	~6.7
(1,1)	1.5687	1.5699	0.7845	54	11	~2.5	~20.4

where $n_2(\lambda), n_1(\lambda)$ are the refractive indexes of fundamental and harmonic of LT crystal, respectively. The participating of the multireciprocal vector leads to the multipeak structure of the spectrum. If m, n are successive Fibonacci numbers, or $(m, n) = (F_{k-1}, F_k)$, the reciprocal vector can be rewritten as $G_{m,n} = G_{s,p} = 2\pi D^{-1} s\tau^p$, where s, p are integers, and $G_{s,p} = G_{s,p-1} + G_{s,p-2}$, thus the $G_{s,p}$ is self-similar. However, because of the dispersion effect, although $G_{s,p}$ presents the self-similarity in reciprocal space, the relation $(1/\lambda)_{s,p+1} = (1/\lambda)_{s,p} + (1/\lambda)_{s,p-1}$ will no longer hold. By careful analysis to the measured spectrum, we do find $(1/\lambda)_{1,4} \neq (1/\lambda)_{1,2} + (1/\lambda)_{1,3}$. This differs from the x-ray diffraction and Raman spectra of quasiperiodic superlattice [4] in which the spectrum structures exhibit self-similarity. Moreover, Eq. (3) can be rewritten as

$$\left[\frac{I}{\lambda}\right]_{s,p} = \frac{s\tau^2}{4[n_2(\lambda) - n_1(\lambda)](1+\tau)l}. \qquad (4)$$

The equation shows that the position of peak (or wavelengths of phase matching) depends on the structure parameter l, and does not depend on the thickness of blocks A and B and their ratio. Figure 2(b) shows the result of numerical calculation for the QPOS of LT with $l = 11$ μm and $l_A/l_B = 1.37$. Indeed from Figs. 2(a) and 2(b) we find a close correspondence between the calculated and measured results on the positions and intensities of peaks. For $l_A/l_B = \tau$, calculation has also shown the positions of corresponding peaks remain unchanged, except for their strengths.

The intensities of peaks in Fig. 2 are related to the effective nonlinear coefficients $d_{m,n}$. Fourier transferring Eq. (2), we can get

$$d_{m,n} = d_{33} \frac{\sin\left(\frac{1}{2} G_{m,n} l\right)}{\frac{1}{2} G_{m,n} l} * \frac{\sin X_{m,n}}{X_{m,n}}; \qquad (5)$$

here $X_{m,n} = \pi D^{-1}\tau^2(ml_A - nl_B)$. For a plane-wave interaction, ignoring depletion of the fundamental field, the second harmonic intensity can be written as [14]

$$I_{2\omega} = \frac{8\pi^2 d_{m,n}^2 L^2 I_\omega^2}{n_1^2 n_2 c\varepsilon_0 \lambda^2} \operatorname{sinc}^2\left(\frac{1}{2}\Delta kL\right), \qquad (6)$$

where LI_ω is the length-intensity product associated with a particular device geometry; n_1, n_2 are the refractive indices of the fundamental and harmonic, respectively; λ is the fundamental wavelength; c is the speed of light; and ε_0 is the dielectric constant of vacuum. When the phase matching condition is satisfied ($\Delta k = 0$), the sinc factor in Eq. (6) is unity. The intensities of peaks are proportional to the square of $d_{m,n}$. In Eq. (5), $d_{m,n}$ contains the two factors $\frac{\sin(1/2G_{m,n}l)}{1/2G_{m,n}l}$ and $\frac{\sin X_{m,n}}{X_{m,n}}$. For $\frac{\sin(1/2G_{m,n}l)}{1/2G_{m,n}l}$, the smaller the indexes m and n, the larger its value. While the value of $\frac{\sin X_{m,n}}{X_{m,n}}$ depends strongly on the indices m, n and the ratio l_A/l_B, $\frac{\sin X_{m,n}}{X_{m,n}}$ is larger when the ratio n/m is closer to ratio l_A/l_B. We calculated the magnitude of the main $d_{m,n}$, for $l_A/l_B = 1.37$ and $l_A/l_B = \tau$ according to Eq. (5); the results are shown in Table II. If $l_A/l_B = \tau$, it is well known that the best rational approximations to τ occur when n and m are successive Fibonacci numbers F_k. The larger $d_{m,n}$ corresponds to $(m, n) = (F_{k-1}, F_k)$. However, this does not mean that the $d_{m,n}$ has the largest value when $l_A/l_B = \tau$. The magnitude of $d_{m,n}$ changes with the ratio of l_A/l_B. The calculated values versus the ratio l_A/l_B from 1 to 2 for some $d_{m,n}$ are shown in Fig. 3. The curves in Fig. 3 show that $d_{m,n}$ with low indices, such as $d_{1,1}, d_{1,2}, \ldots$ exhibit a monotonic dependence on the ratio l_A/l_B in this range, whereas those with high indices, for example $d_{2,3}, d_{3,4}, \ldots$ oscillate in the same range. From Table II and Fig. 3 we can find the two cases for which $d_{m,n} = 0$.

TABLE II. The effective nonlinear coefficients $d_{m,n}$ of quasiperiodic poling $LiTaO_3$.

		$\lvert d_{m,n}/d_{33}\rvert$	
m,n	s,p	$l_A/l_B = 1.37$	$l_A/l_B = \tau$
0,1	1,1	0.156	0.286
1,1	1,2	0.546	0.447
1,2	1,3	0.138	0.195
2,3	1,4	0.184	0.191
3,5	1,5	0.018	0.052
3,4		0.098	0.048
4,3		0.001	0.020
2,2		0	0
4,4		0	0

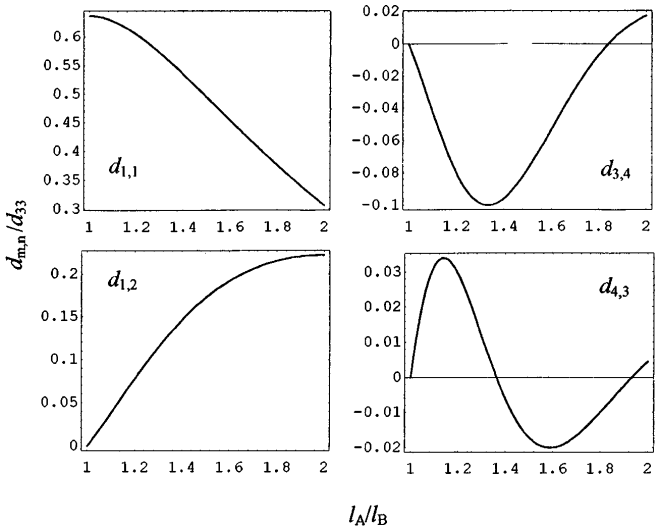

FIG. 3. The dependence of the effective nonlinear coefficients $d_{m,n}$ on the ratio of l_A and l_B.

One is $(m, n) = (2j, 2j)$, in which j is an integer, which corresponds to that the structure parameter l equals an even number times the coherence length of SHG. The other is when the ratio l_A/l_B equals a specified value, e.g., $l_A/l_B = 1.36$ for $G_{3,4}$, which lead to $X_{4,3} = 2\pi$, and $\sin X_{4,3} = 0$. Thus all peaks, with indices (m, n) in accord with the two conditions above will disappear in the spectrum if even the condition of phase matching $\Delta k = 0$ is satisfied. In Fig. 2 the peaks indexed $(2, 2)$ and $(4, 3)$ do not appear in both calculated and measured spectra because these two peaks satisfy extinction conditions: $d_{2,2} = 0$ and $d_{4,3} \approx 0$ for $l_A/l_B = 1.37$, respectively. Since $d_{m,n}$ is a function of ratio l_A/l_B, we may significantly increase some $d_{m,n}$ by optimizing the structure design.

In Table I, we present the values of full width at half maximum (FWHM) of the SHG signal for various phase-matching wavelengths. They are close to the values predicated by theory, which shows that the effective interaction is over the entire sample length in the SHG process. This verifies that the sample was poled uniformly.

We can compare the conversion efficiency $\eta_{m,n}$ of a QPOS with the η_n of a POS through comparing $d_{m,n}$ with d_n. In main $d_{m,n}$, $d_{1,1}$ is maximum, for $l_A/l_B = 1.37, d_{1,1} \approx 0.55 d_{33}$. In contrast with the largest effective nonlinear coefficient of a POS in the first-order QPM, $d_1 = 0.64 d_{33}$. For the equal length-strength parameter LI_ω, the conversion efficiency $\eta_{1,1} \approx 0.75\eta_1$, which is 75% of a POS in a first-order QPM process. The rest is comparable with the third-order QPM's $d_3 \approx 0.2 d_{33}$ (see Table II). This can also be seen from Fig. 3. When the ratio $l_A/l_B \to 1, d_{1,1} \to d_1 = 2d_{33}/\pi$, the rest $\to 0$, thus the system becomes a periodic superlattice, and the multipeak structure in the spectrum will disappear.

In summary, a one-dimensional QPOS of LT consisting of positive and negative ferroelectric domain with Fibonacci sequence has been fabricated using the pulse field poling technique at room temperature. The second harmonic spectrum of the superlattice has been studied theoretically and experimentally. The spectrum does not exhibit self-similarity because of the dispersion of the refractive index of LT. This is in contrast to the x-ray diffraction and Raman spectra of quasiperiodic superlattices in which spectrum structure reflects the symmetry of the quasiperiodic structure. The extinction phenomenon has also been verified experimentally. Frequency conversion efficiencies as high as 5%–20% for SHG at some fundamental wavelengths were measured using a ps-OPO laser, which efficiencies are comparable with that of a POS. Our results show the QPOS may be applied to some multiwavelength SHG devices.

This work was supported by a grant for the Key Research Project in Climbing Program from the National Science and Technology Commission of China. The authors acknowledge assistance in the experiments by P. N. Wang, Q. Guo, and Z. N. Wang of the Anhui of the Institute of Fine Mechanics and Optics.

[1] D. Shechtman, I. Blech, D. Gratias, and J. W. Cahn, Phys. Rev. Lett. **53**, 1951 (1984).
[2] *The Physics of Quasicrystals*, edited by P. J. Steinhardt and S. Ostlund (World Scientific, Singapore, 1987).
[3] C. Janot, *Quasicrystals* (Clarendon Press, Oxford, 1992).
[4] R. Merlin, K. Bajema, and R. Clarke, Phys. Rev. Lett. **55**, 1768 (1985).
[5] A. Behrooz *et al.*, Phys. Rev. Lett. **57**, 368 (1986).
[6] W. Gellermann, M. Kohmoto, B. Sutherland, and P. C. Taylor, Phys. Rev. Lett. **72**, 633 (1994).
[7] R. W. Peng, A. Hu, and S. S. Jiang, Appl. Phys. Lett. **59**, 2512 (1991).
[8] Y. Y. Zhu, N. B. Ming, and W. H. Jiang, Phys. Rev. B **40**, 8536 (1989).
[9] W. Gellermann, M. Kohmoto, B. Sutherland, and P. C. Taylor, Phys. Rev. Lett. **72**, 633 (1994).
[10] Y. Y. Zhu and N. B. Ming, Phys. Rev. B **42**, 3676 (1990).
[11] J. A. Armstrong *et al.*, Phys. Rev. **127**, 1918 (1962).
[12] D. Levine and P. J. Steinhardt, Phys. Rev. B **34**, 596 (1986).
[13] S. N. Zhu *et al.*, J. Appl. Phys. **77**, 5481 (1995).
[14] A. Yariv and P. Yeh, *Optical Wave in Crystal* (Wiley, New York, 1984), pp. 504–551.